Stability of the Lithium "Waterfall" First Wall Protection Concept for Inertial Confinement Fusion Reactors

P.D. Esser, D.D. Paul, and S.I. Abdel-Khalik

August 1980

UWFDM-369

FUSION TECHNOLOGY INSTITUTE

UNIVERSITY OF WISCONSIN

MADISON WISCONSIN

Stability of the Lithium "Waterfall" First Wall Protection Concept for Inertial Confinement Fusion Reactors

P.D. Esser, D.D. Paul, and S.I. Abdel-Khalik

Fusion Technology Institute
University of Wisconsin
1500 Engineering Drive
Madison, WI 53706

http://fti.neep.wisc.edu

August 1980

UWFDM-369

STABILITY OF THE LITHIUM "WATERFALL" FIRST WALL PROTECTION CONCEPT FOR INERTIAL CONFINEMENT FUSION REACTORS

P.D. Esser*, D.D. Paul, and S.I. Abdel-Khalik

Fusion Engineering Program
Nuclear Engineering Department
University of Wisconsin
Madison WI 53706

August 1980

UWFDM-369

This paper submitted for publication in Nuclear Technology.

---

* Presently with Commonwealth Edison Company, Chicago IL.

ABSTRACT

Uncertainties regarding the feasibility of using an annular "waterfall" of liquid lithium to protect the first wall in inertial confinement fusion (ICF) reactor cavities have prompted a theoretical investigation of annular jet stability. Infinitesimal perturbation techniques are applied to an idealized model of the jet with disturbances acting upon either or both of the free surfaces. Dispersion relations are derived which predict the range of disturbance frequencies leading to instability, as well as the perturbation growth rates and jet breakup length. The results are extended to turbulent annular jets and are evaluated for the lithium "waterfall" design. It is concluded that inherent instabilities due to turbulent fluctuations will not cause the jet to break up over distances comparable to the height of the reactor cavity.

NOMENCLATURE

English

$a_{1,2}$	inner and outer radii of unperturbed jet
b	thickness of unperturbed jet
D	diameter
D_e	equivalent diameter
$F_{1,2}$	specified constants
g	gravitational acceleration
i	arbitrary dimensional variable (r, θ , or z)
I_m	modified Bessel function of first kind, order m
j	arbitrary dimensional variable (r, θ , or z)
$k_{1,2}$	wave numbers of inner and outer surface perturbations
K_m	modified Bessel function of second kind, order m
ℓ	Prandtl mixing length
$m_{1,2}$	angular perturbation modes for inner and outer surfaces
n	subscript for jet surface designation ('1' refers to inner surface, '2' refers to outer surface)
n_j	outward pointing unit normal vector in direction j
$n_{1,2}$	number of inner and outer surface wavelengths in control volume
q^2	sum of squares of velocity components ($= u_r^2 + u_\theta^2 + u_z^2$)

r	radial distance
$r_{1,2}$	local inner and outer radii of perturbed jet
S	surface area
t	time
t_B	breakup time
$\vec{u}$	velocity vector
u_i	velocity component in direction i
V	volume
w_o	uniform axial velocity of unperturbed jet
We	Weber number based on equivalent jet radius
$X_{1,2}$	dimensionless perturbation growth frequencies for inner and outer surfaces
z	axial distance
z_B	breakup length
$z_{1,2}$	axial height of control volume

Greek

α	aspect ratio ($= a_1 / a_2$)
$\alpha_{om1,om2}$	initial amplitudes of inner and outer surface perturbations
$\alpha_{m1,m2}$	amplitudes of inner and outer surface perturbations
δp	perturbation pressure
$\eta_{1,2}$	dimensionless wave numbers of inner and outer surface perturbations

θ	angular direction
κ_n	curvature of normal plane
κ_o	curvature of osculating plane
$\lambda_{1,2}$	wavelengths of inner and outer surface perturbations
ρ	density
σ	surface tension
τ_{ij}	stress tensor
$(\tau_{rr})_{1,2}$	normal radial stress component at inner and outer surfaces
ϕ	total velocity potential
ϕ_o	velocity potential of unperturbed jet
$\phi'_{1,2}$	velocity potentials for inner and outer surface perturbations
ψ	phase angle between inner and outer surface perturbations at $z = 0$
$\omega_{1,2}$	growth frequencies for inner and outer surface perturbations

Notes

1. The subscript 'o' refers to the unperturbed jet; the subscript '1' refers to the inner surface of the jet; the subscript '2' refers to the outer surface of the jet.

2. Dots above variables denote differentiation with respect to time; primes denote differentiation with respect to r .

I. INTRODUCTION

The Lawrence Livermore Laboratory has recently brought forth a conceptual design of a laser-driven fusion power plant which uses a vertical, free-falling annular jet, or "waterfall", of liquid lithium to shield the first structural wall from the photons and ions produced by the exploding targets (1,2,3). The explosions take place at a frequency of 1 Hz in the center of a cylindrical cavity into which the annular lithium jet flows downward. The reactions produce energetic neutrons, alpha particles, photons, and other ionic debris which impact onto the lithium fall. The x-rays and ions deposit their energies in the lithium fall, which serves as the primary heat transport and tritium breeding medium. In addition, most of the neutrons' energy is deposited in the fall so that wall damage by high energy neutrons is considerably reduced. The energy deposition, vaporization, and shock waves produced by the microexplosions cause the jet to momentarily disassemble. Recirculating flow through the top of the cavity reestablishes the lithium flow after each explosion.

Among the many uncertainties associated with this concept is the problem of jet stability between explosions (4). Disturbances covering a wide range of frequencies may be caused by a number of factors, including residual pressure pulses and shock waves, nozzle defects, turbulence, and vibration of the reactor housing. The effects of these destabilizing influences,

together with the attendant possibility of jet breakup, constitute the primary motivation for the theory presented in this paper.

In Section II, stability criteria for an idealized laminar annular jet are presented. The derivation follows a linearized, superposition technique. The closed-form solutions are extended to turbulent flow situations in Section III. These results are applied to the lithium "waterfall" concept for ICF reactors in Section IV. Conclusions and recommendations are given in Section V.

II. STABILITY THEORY FOR IDEAL ANNULAR JETS

The pioneering work on the stability of idealized cylindrical liquid jets was performed by Lord Rayleigh (5,6), and was subsequently extended by a number of other investigators. More recently, Anno (7) developed a new "macroscopic" approach to the stability problem. This method, when combined with a number of fundamental assumptions outlined by Paul (8), is readily adaptable to the question of annular jet stability. Here, a stability theory for an ideal annular jet is presented along with the underlying assumptions. A more complete and detailed discussion is furnished by Esser (9).

Consider a section of an annular jet as sketched in Figure 1. In general, the jet is acted upon by disturbances at both its inner and outer free surfaces. The broken lines represent the unperturbed jet, while the solid lines indicate the deformed surfaces. Assume that these surfaces can be defined by the equations:

$$r_1 = a_1 + \alpha_{m1}(t) \cos m_1\theta \cos(k_1 z + \gamma) \qquad (1a)$$

$$r_2 = a_2 + \alpha_{m2}(t) \cos m_2\theta \cos k_2 z \qquad (1b)$$

The cosine representations are actually quite general, since by Fourier's hypothesis any continuous waveform can be represented by summation of a suitable number of sinusoidal components. The idealized jet is characterized by the following assumptions and restrictions:

1. The unperturbed jet is assumed to be an annular vertical liquid jet with uniform, steady, laminar, irrotational, incompressible, and inviscid flow field.
2. The flow field for the perturbed jet is assumed to be three-dimensional, unsteady, laminar, irrotational, incompressible, and inviscid.
3. Linear, superposition analysis is used so that the total perturbation is determined by superposition of the disturbances at the inner and outer free surfaces.
4. Infinitesimal initial axial and angular perturbations are assumed.
5. Mechanical energy effects are considered only; thermal effects are ignored.
6. Gravitational body force only is included.

Now assume a velocity potential of the following form:

$$\phi = \phi_0 + \phi_1' + \phi_2' \qquad (2)$$

where ϕ_o is the component for the unperturbed jet, and is equal to $w_o z$. To find the perturbation terms ϕ_r' and ϕ_z' , the continuity equation is combined with the relationship between velocity and potential to give the Laplacian equations:

$$\frac{1}{r}\frac{\partial}{\partial r}\left(r\frac{\partial \phi_n'}{\partial r}\right) + \frac{1}{r^2}\frac{\partial^2 \phi_n'}{\partial \theta^2} + \frac{\partial^2 \phi_n'}{\partial z^2} = 0 \qquad (3)$$

The subscript n denotes either the inner (n = 1) or outer (n = 2) surface. Equations (3) are solved by separation of variables with two general boundary conditions. The first condition requires that the perturbation velocity components derived from the velocity potential in Equation (2) must equal the time derivatives of the disturbance waveforms in Equations (1). Accordingly, the displacement amplitudes are assumed to vary exponentially with time:

$$\alpha_{mn} = \alpha_{omn} e^{\omega_n t} \qquad (4)$$

The second condition stipulates that a disturbance acting upon one free surface of the jet vanishes at the other surface. This assumption is reflected in the analysis through the perturbation momentum equation for the idealized jet:

$$\rho \left[\frac{\partial \vec{u}}{\partial t} \right]_n = - \left[\text{grad} \, (\delta p) \right]_n \qquad (5)$$

If a disturbance occurs on one free surface of the jet, Equation (5) is applied to the <u>other</u> free surface, and the local perturbation pressure δp is set equal to zero. The resulting solution of Equation (4) yields the second required boundary condition.

Following this approach, Equations (3) are solved and converted to velocity components to give the results:

$$u_r = \frac{\dot{\alpha}_{m1}}{F_1} \left[I'_{m1}(k_1 r) K_{m1}(k_1 a_2) - K'_{m1}(k_1 r) I_{m1}(k_1 a_2) \right] \times$$

$$\times \cos m_1 \theta \cos (k_1 z + \psi) +$$

$$+ \frac{\dot{\alpha}_{m2}}{F_2} \left[I'_{m2}(k_2 r) K_{m2}(k_2 a_1) - K'_{m2}(k_2 r) I_{m2}(k_2 a_1) \right] \times \qquad (6)$$

$$\times \cos m_2 \theta \cos k_2 z$$

$$u_\theta = -\frac{m_1 \dot{\alpha}_{m1}}{r k_1 F_1}\left[I_{m1}(k_1 r) K_{m1}(k_1 a_2) - K_{m1}(k_1 r) I_{m1}(k_1 a_2)\right] \times$$

$$\times \sin m_1\theta \cos(k_1 z + \gamma) -$$

$$- \frac{m_2 \dot{\alpha}_{m2}}{r k_2 F_2}\left[I_{m2}(k_2 r) K_{m2}(k_2 a_1) - K_{m2}(k_2 r) I_{m2}(k_2 a_1)\right] \times \qquad (7)$$

$$\times \sin m_2\theta \cos k_2 z$$

$$u_z = W_o -$$

$$- \frac{\dot{\alpha}_{m1}}{F_1}\left[I_{m1}(k_1 r) K_{m1}(k_1 a_2) - K_{m1}(k_1 r) I_{m1}(k_1 a_2)\right] \times$$

$$\times \cos m_1\theta \sin(k_1 z + \gamma) - \qquad (8)$$

$$- \frac{\dot{\alpha}_{m2}}{F_2}\left[I_{m2}(k_2 r) K_{m2}(k_2 a_1) - K_{m2}(k_2 r) I_{m2}(k_2 a_1)\right] \times$$

$$\times \cos m_2\theta \sin k_2 z$$

where:

$$F_1 = I'_{m1}(k_1 a_1) K_{m1}(k_1 a_2) - K'_{m1}(k_1 a_1) I_{m1}(k_1 a_2) \qquad (9a)$$

$$F_2 = I'_{m2}(k_2 a_2) K_{m2}(k_2 a_1) - K'_{m2}(k_2 a_2) I_{m2}(k_2 a_1) \qquad (9b)$$

(The primes represent differentiation with respect to r.)

The next step in the analysis is specification of the normal stress components, which arise from surface tension forces, acting on the free surfaces of the jet. The derivation of the stress components is given in Appendix A. The results are summarized below:

$$(\tau_{rr})_1 = \frac{\sigma}{a_1} - \frac{\alpha_{m1}\sigma}{a_1^2}\left(1 - m_1^2 - k_1^2 a_1^2\right) \times \qquad (10a)$$

$$\times \cos m_1\theta \cos(k_1 z + \eta)$$

$$(\tau_{rr})_2 = -\frac{\sigma}{a_2} + \frac{\alpha_{m2}\sigma}{a_2^2}\left(1 - m_2^2 - k_2^2 a_2^2\right) \times \qquad (10b)$$

$$\times \cos m_2\theta \cos k_2 z$$

These relationships, together with the velocity components obtained earlier, are applied to the mechanical energy conservation equation written in control volume form. For the idealized annular jet, a macroscopic energy balance can be expressed as follows (Reference (7)):

$$\int_S \tau_{ij} u_i n_j \, dS - \int_S \frac{1}{2} \rho q^2 u_j n_j \, dS - \\ - \int_V \frac{\partial}{\partial t} \frac{1}{2} \rho q^2 \, dV + \int_V \rho g u_z \, dV = 0 \qquad (11)$$

The control volume consists of a length of the unperturbed jet, which is an annular cylinder of inner radius a_1 and outer radius a_2. The length of the control volume is an integral number of disturbance wavelengths on <u>both</u> free surfaces. (For example, the length may be the least common multiple of the two wavelengths that is an integer.) Since the stress tensor and velocity components are dependent on the axial distance z only through sinusoidal functions, the surface integrals taken over the ends of the control volume cancel each other.

Using this control volume, the individual terms of the mechanical energy balance in Equation (11) are evaluated in Appendix B. After simplification, the final result is:

$$\frac{n_1\sigma}{k_1 a_1}\,\alpha_{m1}\dot{\alpha}_{m1} + \frac{n_2\sigma}{k_2 a_2}\,\alpha_{m2}\dot{\alpha}_{m2} =$$

$$= \frac{\rho n_1 a_1}{F_1 k_1^2}\left[K_{m1}(k_1a_1)I_{m1}(k_1a_2) - I_{m1}(k_1a_1)K_{m1}(k_1a_2)\right]\dot{\alpha}_{m1}\ddot{\alpha}_{m1} +$$

$$+ \frac{\rho n_2 a_2}{F_2 k_2^2}\left[I_{m2}(k_2a_2)K_{m2}(k_2a_1) - K_{m2}(k_2a_2)I_{m2}(k_2a_1)\right]\dot{\alpha}_{m2}\ddot{\alpha}_{m2} \qquad (12)$$

(Dots above variables denote differentiation with respect to time.) Since, by Equations (4), α_{m1} and α_{m2} are assumed to vary exponentially with time, Equation (12) can be cast into two separate relations by equating the coefficients of the exponential growth terms. Rearrangement of these equations yields the dispersion relations for the perturbations:

$$\omega_1 = \left\{\frac{\sigma k_1}{\rho a_1^2}\left(1 - m_1^2 - k_1^2 a_1^2\right)\left[\frac{I'_{m1}(k_1a_1)K_{m1}(k_1a_2) - K'_{m1}(k_1a_1)I_{m1}(k_1a_2)}{K_{m1}(k_1a_1)I_{m1}(k_1a_2) - I_{m1}(k_1a_1)K_{m1}(k_1a_2)}\right]\right\}^{1/2} \qquad (13a)$$

$$\omega_2 = \left\{\frac{\sigma k_2}{\rho a_2^2}\left(1 - m_2^2 - k_2^2 a_2^2\right)\left[\frac{I'_{m2}(k_2a_2)K_{m2}(k_2a_1) - K'_{m2}(k_2a_2)I_{m2}(k_2a_1)}{I_{m2}(k_2a_2)K_{m2}(k_2a_1) - K_{m2}(k_2a_2)I_{m2}(k_2a_1)}\right]\right\}^{1/2} \qquad (13b)$$

These results can also be expressed in dimensionless form:

$$X_1 = \left\{ \eta_1 (1 - m_1^2 - \eta_1^2) \left[\frac{I'_{m1}(\eta_1) K_{m1}(\eta_1/\alpha) - K'_{m1}(\eta_1) I_{m1}(\eta_1/\alpha)}{K_{m1}(\eta_1) I_{m1}(\eta_1/\alpha) - I_{m1}(\eta_1) K_{m1}(\eta_1/\alpha)} \right] \right\}^{1/2} \quad (14a)$$

$$X_2 = \left\{ \eta_2 (1 - m_2^2 - \eta_2^2) \left[\frac{I'_{m2}(\eta_2) K_{m2}(\alpha\eta_2) - K'_{m2}(\eta_2) I_{m2}(\alpha\eta_2)}{I_{m2}(\eta_2) K_{m2}(\alpha\eta_2) - K_{m2}(\eta_2) I_{m2}(\alpha\eta_2)} \right] \right\}^{1/2} \quad (14b)$$

where:

$$X_n = \omega_n \left[\frac{\rho a_n^3}{\sigma} \right]^{1/2} \quad (15)$$

$$\eta_n = k_n a_n \quad (16)$$

$$\alpha = \frac{a_1}{a_2} \quad (17)$$

For the particular case where no angular disturbances occur, $m_1 = m_2 = 0$, and the dimensionless dispersion relations become:

$$X_1 = \left\{ \eta_1 (1 - \eta_1^2) \left[\frac{I_1(\eta_1) K_0(\eta_1/\alpha) + K_1(\eta_1) I_0(\eta_1/\alpha)}{K_0(\eta_1) I_0(\eta_1/\alpha) - I_0(\eta_1) K_0(\eta_1/\alpha)} \right] \right\}^{1/2} \quad (18a)$$

$$X_2 = \left\{ \eta_2 (1 - \eta_2^2) \left[\frac{I_1(\eta_2) K_0(\alpha\eta_2) + K_1(\eta_2) I_0(\alpha\eta_2)}{I_0(\eta_2) K_0(\alpha\eta_2) - K_0(\eta_2) I_0(\alpha\eta_2)} \right] \right\}^{1/2} \quad (18b)$$

It can be shown (Reference (9)) that the factors in square brackets in Equations (14) are always positive for $\eta_n > 0$ and $\alpha < 1$. Therefore, $X_1^2 < 0$ and $X_2^2 < 0$ if $m_1 \geq 1$ and $m_2 \geq 1$. In this case the dimensionless growth frequencies are both imaginary, indicating that the jet is stable. However, if $m_1 = m_2 = 0$ (no angular disturbances), the free surfaces may or may not be stable, depending on the values of η_1 and η_2. For this situation, it is seen that $X_n^2 > 0$ for $0 \leq \eta_n < 1$; otherwise $X_n^2 < 0$. Since the amplitudes of the perturbations grow exponentially with time when $X_n^2 > 0$, the jet becomes unstable. When $X_n^2 < 0$, the amplitudes oscillate sinusoidally but the jet remains stable. Instabilities can occur at either or both of the free surfaces. When both surfaces are unstable, the total disturbance is found by superposition of the individual perturbations.

The dispersion relations defined by Equations (18) are plotted in Figures 2 and 3. The limiting values of X_n are nonzero as η_n approaches zero, but vanish as η_n tends toward unity. Furthermore, if the aspect ratio α is less than a particular value, the maximum values of X_n occur in the limit as η_n goes to zero. If α is greater than this value, the maxima occur in the range $0 < \eta_1 < 1$. (The transition aspect ratio values are $\alpha \simeq 0.29$ for the inner free surface and $\alpha \simeq 0.06$ for the outer surface.) A disturbance at a given surface is stable (that is, does not grow with time) if the value of the corresponding wave number η_n is greater than unity.

In Figure 2, the dispersion curve for $\alpha = 0$ is a limiting case which represents the inner surface of an infinite jet with a finite-sized central "hole". The curve agrees with the original analytical result of Lord Rayleigh (10) for this situation. Similarly, the curve for $\alpha = 0$ in Figure 3 represents the surface of a solid cylindrical jet, and also matches the classical findings of Lord Rayleigh (5,6).

Using the stability criteria obtained earlier in this section, it is possible to derive approximate expressions for the jet breakup length. This is defined as the distance along the jet at which the amplitude of a perturbation

becomes comparable to the jet thickness. Considering a disturbance at either free surface, the time at which breakup occurs is found by rearranging Equations (4):

$$t_B = \frac{1}{\omega_n} \ln \left(\frac{b}{\alpha_{omn}} \right) \tag{19}$$

The breakup time is equal to the breakup length divided by the jet speed. Consequently:

$$\frac{Z_B}{W_o} = \frac{1}{\omega_n} \ln \left(\frac{b}{\alpha_{omn}} \right) \tag{20}$$

In dimensionless form:

$$\frac{Z_B}{a_n} = \frac{1}{\sqrt{2}\, X_n} \left[\frac{2 \rho W_o^2 a_n}{\sigma} \right]^{1/2} \ln \left(\frac{b}{\alpha_{omn}} \right) \tag{21}$$

The quantity in square brackets represents an effective Weber number for the jet. Its value depends on the properties of the fluid and the flow characteristics. The value of X_n is read directly from the appropriate graph in Figure 2 or 3. Therefore, if the initial disturbance amplitude α_{omn} is known, the breakup length can be calculated directly from

Equations (21). Application of this result to laminar flow situations is discussed in Reference (9). Turbulent flow cases, which include the annular lithium "waterfall" for ICF reactors, are examined in the next section.

III. STABILITY THEORY FOR TURBULENT ANNULAR JETS

In order to apply the results from ideal laminar theory to turbulent flows, the jet is assumed to exhibit "pseudo-laminar" behavior (Reference (11)). In this case, the disturbance growth rates obey the laminar flow equations, but the instabilities are actually produced by turbulent velocity fluctuations. This laminar analogy has been used with varying degrees of success in the turbulence correlation studies of several researchers (Reference (9)) for solid cylindrical jets. Other possible effects include the characteristics of the ambient surroundings and viscocity of the jet fluid (reflected in the value of the Reynolds number). These influences are, however, ignored in the analysis of the annular lithium "waterfall" for the following reasons. First, the ambient pressure in the reactor cavity is very low (< 0.1 torr), so that external effects should be negligible. Second, it has been shown (Reference (9)) that the viscous effects become very small at the high flow velocities encountered in the jet. Therefore, the remaining parameters which control the stability behavior of the lithium "waterfall" are the initial disturbance level and the jet Weber number.

Phinney (12) reasoned that, in a fully turbulent jet, surface tension acts as a stabilizing influence, damping the disruptions caused by internal turbulent motion. This is opposite to the situation in a purely laminar flow, where surface tension is the primary breakup mechanism. This physical model implies that the dependence of the stability criteria on the frequencies or wavelengths of external disturbances is not valid for the turbulent case. In particular, it may be assumed that inherent instabilities always exist, and that they need not have dimensionless wave numbers in the range of zero to unity in order to promote breakup.

With this information as background, Equations (21) can now be used to make a rough estimate of the breakup length for a turbulent annular jet. The relationship between the jet thickness b and the initial disturbance amplitude α_{omn} is determined by the following approach. Semiempirical studies conducted by Nikuradse (13) indicate that the turbulent eddy of largest size in a circular pipe is characterized by the expression:

$$\frac{\ell}{D} \simeq 0.14 \qquad (22)$$

where ℓ is the Prandtl mixing length and D is the pipe diameter. Assume that this expression remains valid for free turbulent jet flow (Reference (11)), and that D can be replaced by D_e, the equivalent diameter, for the special case of annular flow. If the mixing length corresponds to the eddy size and is taken to be the amplitude of the initial disturbance, then, since $D_e = 2b$:

$$\frac{\alpha_{omn}}{b} \simeq 0.28 \tag{23}$$

Substitution into Equations (21) gives:

$$\frac{z_B}{a_n} \simeq \frac{0.9}{X_n}\left[\frac{2\rho W_o^2 a_n}{\sigma}\right]^{1/2} \tag{24}$$

For the case of the annular lithium "waterfall", Equations (24) must be corrected for the fact that the flow is fully turbulent, and not "pseudo-laminar". The experiments of Phinney (12) with solid cylindrical jets suggest that the results can be applied to turbulent flows if they are multiplied by the following factor:

$$\frac{(z_B)_{turbulent}}{(z_B)_{pseudo-laminar}} \simeq 0.33 + \frac{17}{\sqrt{We}} \qquad (25)$$

Here We is the "true" Weber number of the annular jet, based on the equivalent diameter, and is given by:

$$We = \frac{2 \rho W_o^2 b}{\sigma} \qquad (26)$$

After multiplication by the conversion factor (25), Equations (24) become:

$$\frac{z_B}{a_n} \simeq \frac{0.3}{X_n}\left[\frac{2 \rho W_o^2 a_n}{\sigma}\right]^{1/2} + \frac{15}{X_n}\left[\frac{a_n}{b}\right]^{1/2} \qquad (27)$$

The final step in the analysis is to specify appropriate values for a_n and X_n. Since the random turbulent fluctuations which promote instability occur throughout the jet, neither of the free surfaces is disrupted preferentially. Therefore, since $a_1 < a_2$, Equations (27) indicate that the shortest calculated breakup distance occurs when the disturbance is assumed to evolve from the inside surface ($n = 1$). It follows that this minimum value of z_B is the <u>actual</u> breakup distance. Hence, the final result is:

$$\frac{z_B}{a_1} \simeq \frac{0.3}{X_1}\left[\frac{2\rho W_o^2 a_1}{\sigma}\right]^{1/2} + \frac{15}{X_1}\left[\frac{a_1}{b}\right]^{1/2} \qquad (28)$$

The proper value of X_1 to use in Equation (28) is the maximum, as shown in Figure 2, for a given aspect ratio. This follows from the "narrow-band" statistical theory of Lafrance (14), which asserts that turbulent jet breakup is induced by random perturbations acting on an otherwise laminar jet. Only a narrow range of wave numbers near the maximum (as calculated from laminar stability theory) can participate significantly in the breakup process.

IV. APPLICATION TO ANNULAR LITHIUM "WATERFALL" CONCEPT

The semiempirical expression for the breakup length of a turbulent annular jet, as given in Equation (28), can be applied directly to the case of the liquid lithium "waterfall" first wall protection concept for ICF reactors. Table 1 gives some preliminary design values for the key parameters of the reactor cavity and the lithium flow. From Figure 2, for an aspect ratio of 0.87, $(X_1)_{max} = 2.7$. Inserting this and the other appropriate values from Table 1 into Equation (28), the approximate breakup length for the "waterfall" is 430 m .

This distance is a factor of about 50 greater than the design height of the reactor cavity. Therefore, it is concluded that flow instability due to turbulence poses no significant problems or constraints for this concept. However, in view of the assumptions and approximations tied to this analysis and the lack of experimental data, the result should be looked upon only as a crude, semiquantitative estimate.

V. CONCLUSIONS AND RECOMMENDATIONS

Uncertainties in the flow stability of a conceptual annular liquid lithium "waterfall" for ICF reactors have prompted a general theoretical investigation of annular jet stability. By using a first-order, infinitesimal perturbation approach coupled with superposition and the fundamental assumption that a disturbance at one surface vanishes at the other, closed-form solutions for the perturbation growth rates for idealized laminar jets are obtained. Sinuscidal surface disturbances are stable if their dimensionless wave numbers are greater than unity; otherwise, they grow exponentially with time. Breakup of the jet is dominated by the disturbance with the fastest growth rate. The breakup length of the jet can be determined if the amplitude of the initial perturbation is known.

The results are extended to turbulent flows by applying empirical correlations and a "narrow-band" statistical theory, originally obtained for solid cylindrical jets, through use of the equivalent diameter concept. Semiempirical expressions for breakup length are derived for "pseudo-laminar" and fully turbulent flows. The estimated distance at which the lithium

"waterfall" is expected to disintegrate due to turbulence is 430 m , which is far greater than the design height of the reactor cavity. Consequently, flow stability is not anticipated to be a limiting constraint for this application.

Undoubtedly the present theory can be improved by consideration of additional factors (for example, flow Reynolds number, ambient conditions, finite-amplitude disturbances), and by applying a higher-order method of solution. However, due to the great effort which would be involved, it is felt that these refinements should await the results of a broad experimental program on annular jet stability. A full-scale empirical study of the lithium "waterfall" itself would be a valuable contribution. The results of such experiments may be used to confirm or disprove the fundamental assertions upon which the analytical work is based.

REFERENCES

1. Maniscalco, J.A. and W.R. Meier, "Liquid-Lithium 'Waterfall' Inertial Confinement Fusion Reactor Concept", Trans. Am. Nucl. Soc., 26, 62 (Jun. 1977).

2. Maniscalco, J.A., W.R. Meier, and M.J. Monsler, "Conceptual Design of a Laser Fusion Power Plant", UCRL-79652, Lawrence Livermore Laboratory (Jul. 1977).

3. Meier, W.R. and J.A. Maniscalco, "Reactor Concepts for Laser Fusion", UCRL-79654, Lawrence Livermore Laboratory (Jul. 1977).

4. Abdel-Khalik, S.I., R.W. Conn, and G.A. Moses, "Engineering Problems of Laser-Driven Fusion Reactors", Nucl. Technol., 43, 5 (Apr. 1979).

5. Rayleigh, J.S.W. (Lord), "On the Instability of Jets", Proc. London Math. Soc., 10, 4 (1879).

6. Rayleigh, J.S.W. (Lord), The Theory of Sound, Vol. 2, pp. 351-359, Dover Publications, New York (1945).

7. Anno, J.N., The Mechanics of Liquid Jets, Chap. 3, pp. 19-45, D.C. Heath and Company, Lexington, MA (1977).

8. Paul, D.D., "Dynamics of Newtonian Annular Jets", M.S. Thesis, Nuclear Engineering Department, University of Wisconsin-Madison (Dec. 1978).

9. Esser, P.D., "Theory of Annular Liquid Jet Flow", M.S. Thesis, Nuclear Engineering Department, University of Wisconsin-Madison (May 1980).

10. Rayleigh, J.S.W. (Lord), "On the Instability of Cylindrical Fluid Surfaces", Phil. Mag., 34, 177 (1892).

11. Chen, T.F. and J.R. Davis, "Disintegration of a Turbulent Water Jet", Proc. Am. Soc. Civil Engrs., HY1, 175 (Jan. 1964).

12. Phinney, R.E., "Breakup of a Turbulent Liquid Jet in a Low-Pressure Atmosphere", AIChE Journal, 21, 996 (Sep. 1975).

13. Schlicting, H., Boundary-Layer Theory, 7th ed., Chap. 20, p. 605, McGraw-Hill Book Co., New York (1979).

14. Lafrance, P., "The Breakup Length of Turbulent Liquid Jets", ASME J. Fluids Engr., 99, 414 (Jun. 1977).

APPENDIX A: EVALUATION OF BOUNDARY PRESSURES

Surface tension forces produce a discontinuous difference in pressure between the boundaries of a fluid jet with curved free surfaces and the ambient surroundings. The pressure differential is given by (Reference (7)):

$$\tau_{rr} = \sigma (\kappa_o + \kappa_n) \tag{A1}$$

κ_o is the curvature in the osculating (vertical) plane at the free surface, and κ_n is the curvature in the normal (horizontal) plane. The curvature is considered positive when the fluid is located on the convex side, and negative when it is on the concave side.

The curvature in the osculating plane is, respectively, for the inner and outer free surfaces of an annular jet (Reference (7)):

$$(\kappa_o)_1 = \left(\frac{d^2 r_1}{dz^2}\right)\left[1 + \left(\frac{dr_1}{dz}\right)^2\right]^{-3/2} \tag{A2a}$$

$$(\kappa_o)_2 = -\left(\frac{d^2 r_2}{dz^2}\right)\left[1 + \left(\frac{dr_2}{dz}\right)^2\right]^{-3/2} \tag{A2b}$$

The corresponding curvatures in the normal plane are given by (Reference [7]):

$$(\chi_n)_1 = -\left[r_1^2 + 2\left(\frac{dr_1}{d\theta}\right)^2 - r_1\frac{d^2r_1}{d\theta^2}\right]\left[r_1^2 + \left(\frac{dr_1}{d\theta}\right)^2\right]^{-3/2} \quad \text{(A3a)}$$

$$(\chi_n)_2 = \left[r_2^2 + 2\left(\frac{dr_2}{d\theta}\right)^2 - r_2\frac{d^2r_2}{d\theta^2}\right]\left[r_2^2 + \left(\frac{dr_2}{d\theta}\right)^2\right]^{-3/2} \quad \text{(A3b)}$$

Substituting for r_1 and r_2 from Equations (1) and approximating to first order in α_{m1} and α_{m2} yields:

$$(\chi_o)_1 \simeq -\alpha_{m1} k_1^2 \cos m_1\theta \cos(k_1 z + \psi) \quad \text{(A4a)}$$

$$(\chi_o)_2 \simeq \alpha_{m2} k_2^2 \cos m_2\theta \cos k_2 z \quad \text{(A4b)}$$

$$(\chi_n)_1 \simeq -\frac{1}{a_1} + \frac{\alpha_{m1}}{a_1^2}(1 - m_1^2)\cos m_1\theta \cos(k_1 z + \psi) \quad \text{(A5a)}$$

$$(\mathcal{H}_n)_2 \simeq \frac{1}{a_2} - \frac{\alpha_{m2}}{a_2^2}(1 - m_2^2)\cos m_2\theta \cos k_2 z \qquad \text{(A5b)}$$

Combining Equations (A1), (A4), and (A5) gives, after rearrangement, the expressions shown in Equation (10) of the article.

APPENDIX B: EVALUATION OF TERMS IN MECHANICAL ENERGY EQUATION

As described in the article, the control volume used for the mechanical energy balance is an annular cylinder of inner radius a_1 and outer radius a_2. The length of the control volume is chosen so that it includes an integral number of sinusoidal disturbance wavelengths on <u>both</u> free surfaces. If one end of the control volume is located at $z = 0$, the position of the other end is:

$$z_1 = z_2 = n_1\lambda_1 = n_2\lambda_2 = \frac{2\pi n_1}{k_1} = \frac{2\pi n_2}{k_2} \qquad \text{(B1)}$$

The values of the differential factors in the integrands are:

$$(u_j n_j dS)_1 = -a_1 \dot{\alpha}_{m1} \cos m_1\theta \cos(k_1 z + \psi)\, d\theta\, dz \qquad \text{(B2a)}$$

$$(u_j n_j dS)_2 = a_2 \dot{\alpha}_{m2} \cos m_2\theta \cos k_2 z\, d\theta\, dz \qquad \text{(B2b)}$$

$$dV = r\, d\theta\, dz\, dr \qquad \text{(B3)}$$

The limits of integration are $z = 0$ to $z = z_1 = z_2$, $\theta = 0$ to $\theta = 2\pi$, and (for volume integrals) $r = a_1$ to $r = a_2$.

Consider the first term in Equation (11), which represents energy generation due to surface forces. Since there are no shear stresses and n_j is the outward pointing unit normal vector, $\tau_{ij} = \tau_{rr}$. Substituting for τ_{rr} from Equations (10) and integrating gives:

$$\int_s \tau_{ij}\, u_j\, n_j\, dS = \int_{S_1} (\tau_{rr})_1 (u_r n_r dS)_1 + \int_{S_2} (\tau_{rr})_2 (u_r n_r dS)_2 \qquad (B4)$$

$$= \frac{\pi^2 n_1 \sigma\, \alpha_{m1}\, \dot{\alpha}_{m1}}{k_1 a_1} \left(1 - m_1^2 - k_1^2 a_1^2\right) + \frac{\pi^2 n_2 \sigma\, \alpha_{m2}\, \dot{\alpha}_{m2}}{k_2 a_2} \left(1 - m_2^2 - k_2^2 a_2^2\right) \qquad (B5)$$

Similarly, for the second term in Equation (11):

$$\int_s \tfrac{1}{2} \rho q^2 u_j n_j\, dS = \int_{S_1} \tfrac{1}{2} \rho q^2 (u_r n_r dS)_1 + \int_{S_2} \tfrac{1}{2} \rho q^2 (u_r n_r dS)_2 \qquad (B6)$$

where $q^2 = u_r^2 + u_\theta^2 + u_z^2$. Substituting for the velocity components and performing the indicated operations leads to the result:

$$\int_S \frac{1}{2} \rho q^2 u_j n_j \, dS = 0 \tag{B7}$$

The fact that this term vanishes can be understood on intuitive grounds. The surface integral represents the net efflux of mechanical energy from the control volume. As a result of the spatially periodic, sinusoidal nature of the disturbances, the net outflow of energy must be zero.

The third term in Equation (11) gives the rate of change of kinetic energy within the control volume. A detailed integration is carried out in Reference (9). The result is:

$$\int_V \frac{\partial}{\partial t} \frac{1}{2} \rho q^2 \, dV =$$

$$= \frac{2\pi^2 n_1 a_1 \dot{\alpha}_{m1} \ddot{\alpha}_{m1}}{k_1^2} \left[\frac{K_{m1}(k_1 a_1) I_{m1}(k_1 a_2) - I_{m1}(k_1 a_1) K_{m1}(k_1 a_2)}{I'_{m1}(k_1 a_1) K_{m1}(k_1 a_2) - K'_{m1}(k_1 a_1) I_{m1}(k_1 a_2)} \right] \tag{B8}$$

$$+ \frac{2\pi^2 n_2 a_2 \dot{\alpha}_{m2} \ddot{\alpha}_{m2}}{k_2^2} \left[\frac{I_{m2}(k_2 a_2) K_{m2}(k_2 a_1) - K_{m2}(k_2 a_2) I_{m2}(k_2 a_1)}{I'_{m2}(k_2 a_2) K_{m2}(k_2 a_1) - K'_{m2}(k_2 a_2) I_{m2}(k_2 a_1)} \right]$$

The last term in Equation (11) represents the increase in mechanical energy due to gravity. In evaluating this integral, the unperturbed component of the axial velocity, w_o, is neglected since it is explicitly assumed to remain constant with respect to both space and time. This is admittedly an unrealistic constraint, although its influence diminishes for high speed vertical jets. Substituting the perturbation component of u_z into this term and integrating leads to the result:

$$\int_V \rho g u_z \, dV = 0 \qquad \text{(B9)}$$

Combining Equations (B5), (B7), (B8), and (B9) yields, after rearrangment, the result in Equation (12) of the article.

Table 1: Lawrence Livermore Laboratory ICF Reactor and Lithium "Waterfall" Design Parameters (1,2,3)

Inner Jet Radius	4.0 m
Outer Jet Radius	4.6 m
Jet Thickness at Midplane	0.6 m
Aspect Ratio	0.87
Chamber Height	8.0 m
Inlet Jet Velocity	8.0 m/sec
Jet Reynolds Number	9.8×10^6
Jet Weber Number	1.0×10^5
Chamber Pressure	< 0.1 torr
Reaction Pulse Rate	1.4 Hz
Lithium Temperature	700° K
Lithium Density	490 kg/m^3
Lithium Surface Tension	0.36 N/m
Lithium Viscosity	0.00048 kg/m-sec

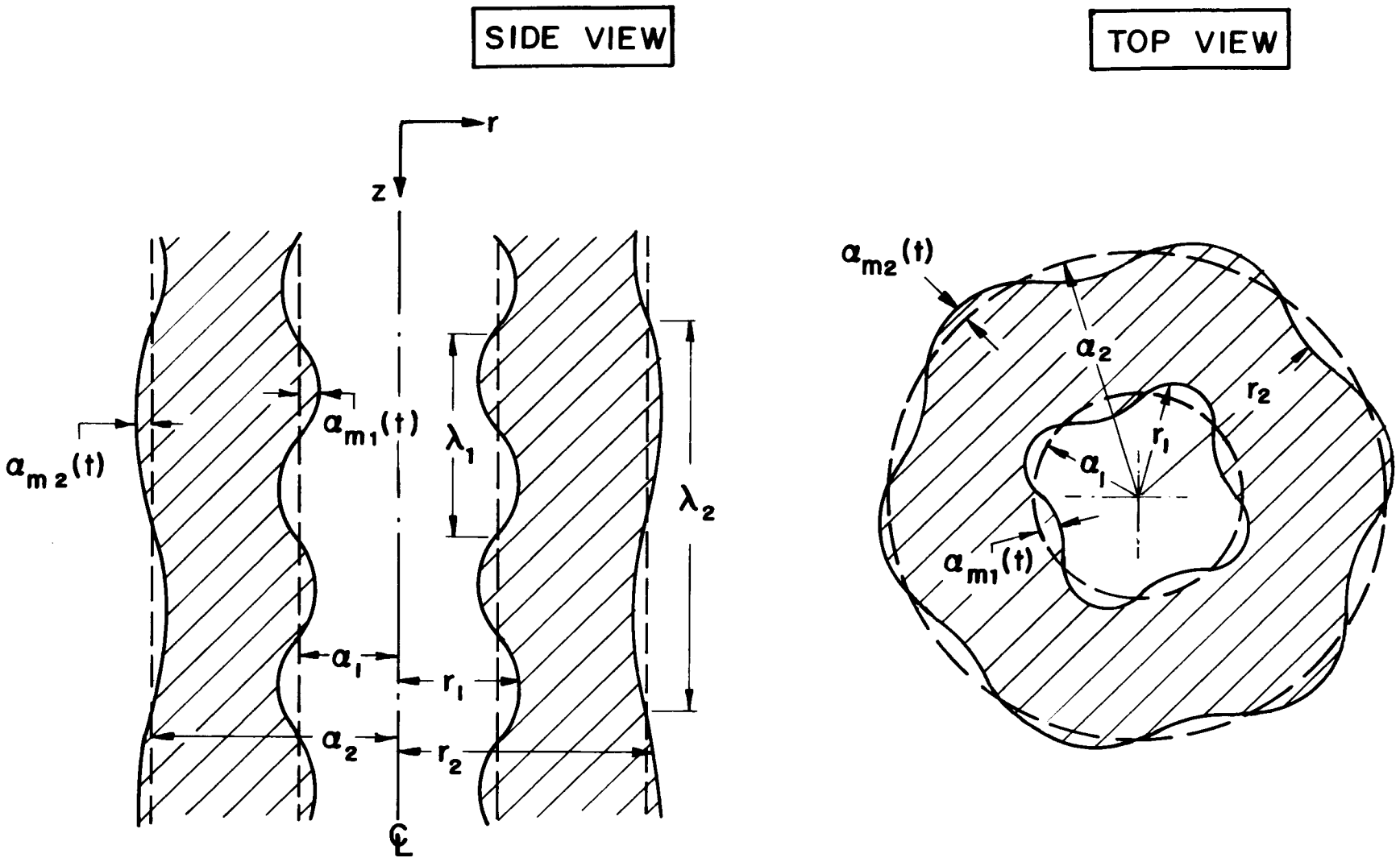

Figure 1: Geometry of an Annular Jet with Axial and Angular Disturbances

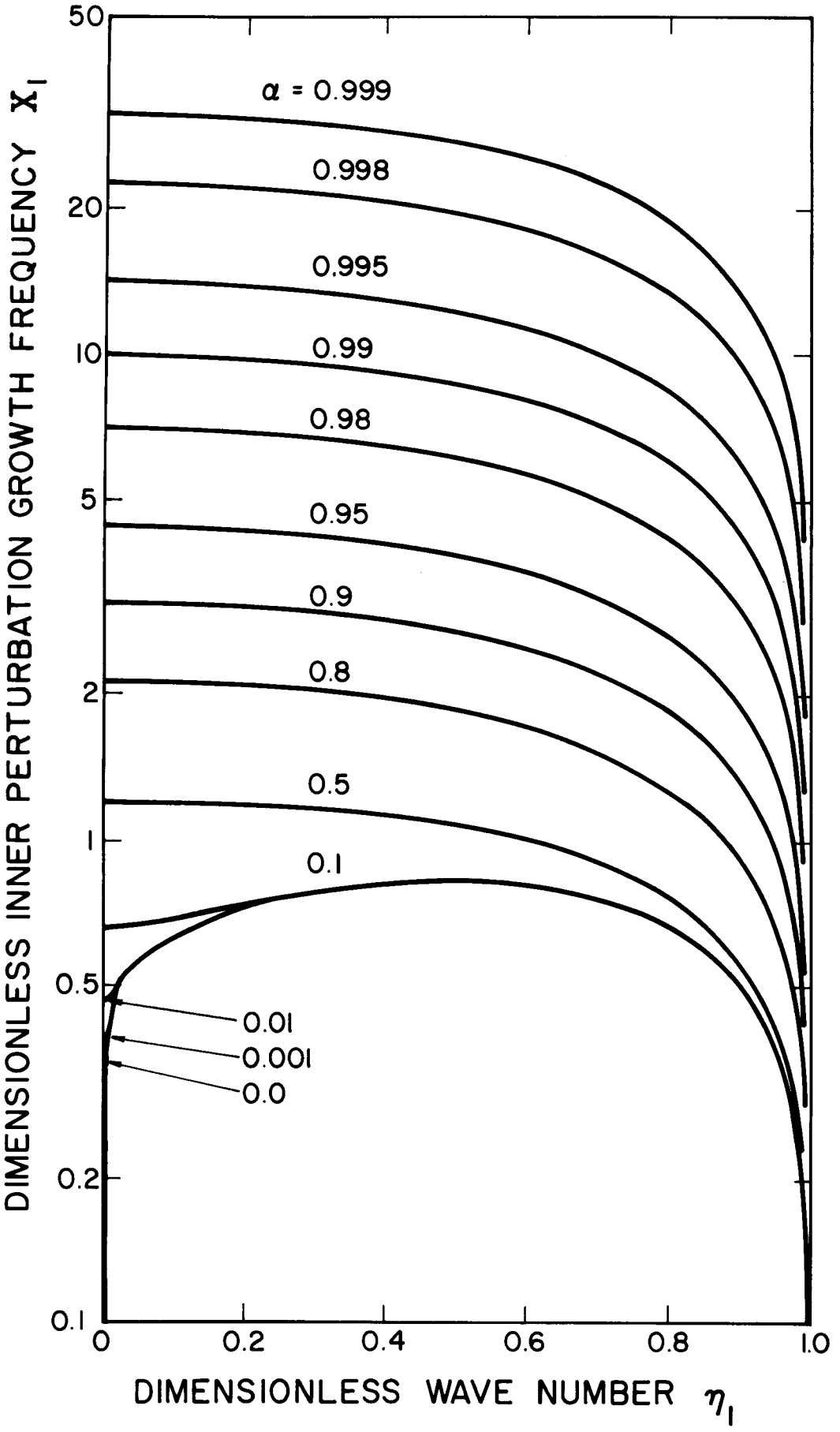

Figure 2: Dimensionless Growth Frequency versus Dimensionless Wave Number for Inner Free Surface

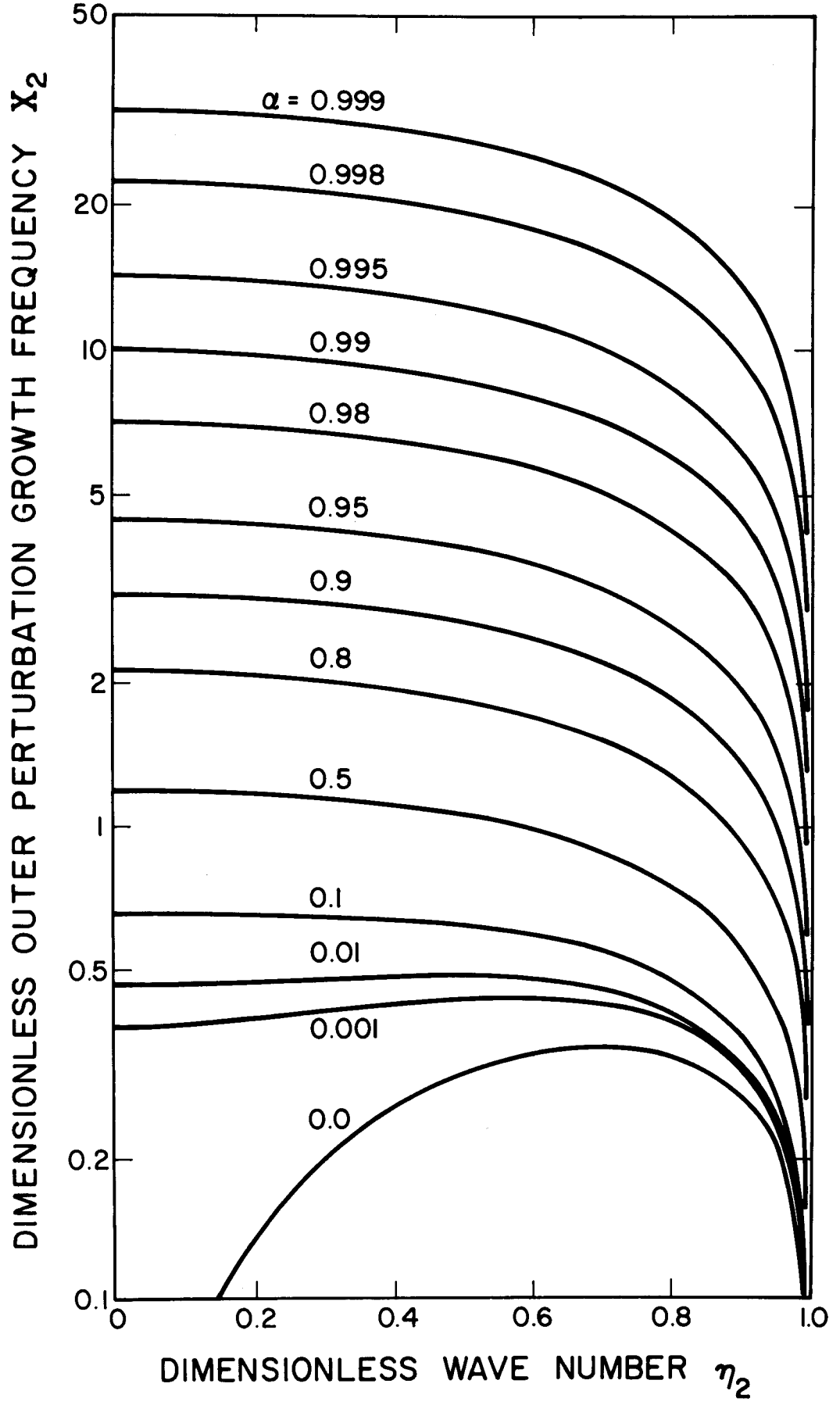

Figure 3: Dimensionless Growth Frequency versus Dimensionless Wave Number for Outer Free Surface